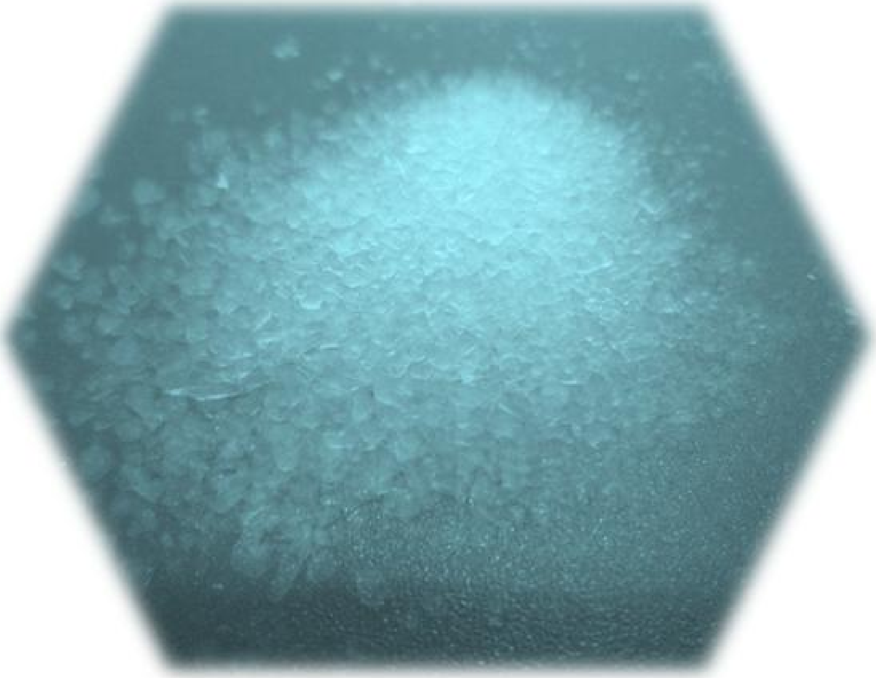

Literature Review of High Performance Thermal Insulation

Report in Building Physics

AXEL BERGE, PÄR JOHANSSON

Department of Civil and Environmental Engineering
Division of Building Technology
Building Physics
CHALMERS UNIVERSITY OF TECHNOLOGY
Gothenburg, Sweden 2012
Report 2012:2

REPORT 2012:2

Literature Review of High Performance Thermal Insulation

Report in Building Physics

AXEL BERGE, PÄR JOHANSSON

Department of Civil and Environmental Engineering
Division of Building Technology
Building Physics
CHALMERS UNIVERSITY OF TECHNOLOGY

Gothenburg, Sweden 2012

Literature Review of High Performance Thermal Insulation

Report in Building Physics

Report / Department of Civil and Environmental Engineering,
Chalmers University of Technology
Report 2012:2
ISSN 1652-9162

Department of Civil and Environmental Engineering
Division of Building Technology
Building Physics
Chalmers University of Technology
SE-412 96 Gothenburg, Sweden
Telephone: + 46 (0)31-772 1000

Cover:
Silica aerogel granulates. The production process and physical properties of the aerogel are described in Chapter 3 (Photo: Axel Berge).

Department of Civil and Environmental Engineering
Gothenburg, Sweden 2012

Literature Review of High Performance Thermal Insulation
Report in Building Physics
AXEL BERGE, PÄR JOHANSSON
Department of Civil and Environmental Engineering
Division of Building Technology
Building Physics
Chalmers University of Technology

ABSTRACT

The European Union has decided to decrease the energy use for heating of buildings with 50% in 2050. To reach the target the amount of insulation in the building envelope has to increase. With conventional insulation materials, such as mineral wool and expanded polystyrene (EPS), the required additional thickness of the building envelope leads to a larger share of the building area dedicated for structural elements. A number of high performance thermal insulation materials and components have been introduced to the building market during the last decades which can give the same thermal resistance using a thinner construction. This report presents how insulation materials work. The properties of aerogels and vacuum insulation panels (VIP) are described more in detail.

Heat transfer in thermal insulation materials is generally divided in heat conduction through the solid material, conduction through the gas molecules and radiation through the pores. Gas convection in the material can be important on a larger material scale and in porous materials, such as mineral wool. Aerogel for building applications has a thermal conductivity of around 14-16 mW/(m·K) while VIP can reach down to 4 mW/(m·K). This can be compared to EPS and stagnant air with a thermal conductivity of 36 and 25 mW/(m·K) respectively. Aerogel and VIP have small pores in the range of 10-100 nm which means the gas conductivity is reduced at atmospheric pressure.

Up till now aerogel has been used in space industry, chemical industry and in sport equipment but not that much in buildings. A limiting factor is the high cost of the aerogel. Since the end of the 1990s VIP has been used in buildings but originally they were developed for refrigerators and cold shipping boxes. To use VIP in buildings, the architects and engineers have to pay special attention to attachment details since the VIP cannot be adapted on the construction site. Nevertheless, novel high performance thermal insulation materials could be an important and feasible solution to decrease the thickness of the building envelope while maintaining the thermal resistance. These materials create new opportunities for architects and engineers to design energy efficient buildings.

Key words: thermal insulation material, heat transfer, aerogel, vacuum insulation panel, building

Contents

Preface

This study is based on research papers, conference papers and reports which have been gathered to give a basis for the thermal and physical properties of conventional and novel high performance thermal insulation materials and components. The report was produced at the Division of Building Technology, Building Physics Research group, at Chalmers University of Technology in Gothenburg, Sweden. The study was financed by FORMAS, the Swedish Research Council for Environment, Agricultural Sciences and Spatial Planning through the projects "Retrofit applications on old buildings using highly efficient novel thermal insulation materials" and "Homes for tomorrow (h42): Building solutions for tomorrow as a reference for today".

There is a number of different thermal insulation materials used in the building industry today. Conventional materials, such as glass wool, rock wool, expanded polystyrene (EPS) and extruded polystyrene (XPS), require a thick building envelope to reach a sufficiently low thermal transmittance. When energy retrofitting old buildings a number of factors, such as the limited space and protected features of the façade, has to be taken into account to reduce the energy use. In the near future novel high performance thermal insulation materials and components create new opportunities for architects and engineers to design energy efficient buildings.

Gothenburg, June 2012

Axel Berge and Pär Johansson

Notations and abbreviations

Roman letters

c	(J/(kg·K))	Specific heat capacity
d	(m)	Thickness
g	(m/s^2)	Gravitational acceleration
k	(m^2)	Permeability
k_B	(J/K)	Boltzmann constant
l_{mean}	(m)	Mean free path
n	(-)	Refraction index
q	(W/m^2)	Heat flux
A	(m^2)	Area
K	(-)	Extinction coefficient
K_n	(-)	Knudsen number
Nu	(-)	Nusselt number
P_g	(Pa) or (bar)	Gas pressure
Ra_m	(-)	Modified Rayleigh number
T	(°C) or (K)	Temperature
$\dot{V}$	(m^3/s)	Volume flow

Greek letters

β_a	(-)	Heat transfer efficiency between gas molecule and pore wall
β	(1/K)	Thermal expansion coefficient for air
δ	(m)	Characteristic size of a system
ε	(-)	Emissivity
λ	(W/(m·K))	Thermal conductivity
μ	(kg/(m·s))	Dynamic viscosity
v	(m^2/s)	Kinematic viscosity
ρ	(kg/m^3)	Density
σ	(J/(K^{4}m^{2}s))	Stefan-Bolzmann constant
Ψ	(W/(m·K))	Linear thermal transmittance coefficient

Abbreviations

DIM	Dynamic insulation material	OTR	Oxygen transmission rate
EPS	Expanded polystyrene	PIR	Polyisocyanurate
HCN	Hydrogen cyanide	PUR	Polyurethane
HFC	Hydroflourocarbons	VIM	Vacuum insulation material
GFP	Gas filled panel	VIP	Vacuum insulation panel
GIM	Gas insulation material	WVTR	Water vapor transmission rate
NIM	Nano insulation material	XPS	Extruded polystyrene

1 Introduction

The energy use in the European Union should decrease with 20% in 2020 and with 50% in 2050 compared to the energy use in 1990 (European Commission, 2008). A large part of the energy use is related to heating of buildings and production of domestic hot water. In Sweden, this part is just below 30% of the total end energy use which corresponds to around 10% of the Swedish greenhouse gas emissions. The data on energy use is uncertain, but according to the Swedish National Board of Housing, Building and Planning (Boverket) which is responsible for the Swedish energy use targets in buildings, the energy use for heating and domestic hot water has been reduced by 8% between 1995 and 2008. To reach the Swedish energy use targets of a 20% reduction in 2020 and a 50% reduction to 2050 compared to 1995, further decisive actions are needed (Boverket, 2010).

The Montreal protocol from 1987 that went in force in 1989 demanded a phase out of the worst ozone depleting gases till 1996. Thermal insulation materials, such as polyurethane (PUR) foam, were filled with these substances which demanded research on how to replace them in thermal insulation materials. In the late 1980s and early 1990s the research was focused mainly on replacing the materials with the ozone depleting CFC-11 (trichlorofluoromethane) (Brodt, 1995). New materials and components have been introduced to the market, such as cellulose fiber insulation, foamglass, polyurethane (PUR), polyisocyanurate (PIR), expanded polystyrene (EPS) with added graphite, aerogel and vacuum insulation panels (VIP).

When introducing new materials to the market, it is very important not only to look at the physical properties of the material as such, but also to compare the way of manufacturing and recycling the material. It is important to ensure that no rebound effects occur when changing to a more efficient material that could be more energy demanding in the manufacturing process. This study focuses on the application of aerogel and VIP since these are the components that without comparison have the highest potential for energy-efficient building applications today.

2 Heat transfer in insulation materials

The function of insulation materials is to minimize the transport of heat through the construction. The heat transport can normally be divided in three parts; conduction through solid, conduction through gas phase and radiation through pores as shown in Equation (2.1).

$$\lambda_{tot} = \lambda_{gas} + \lambda_{solid} + \lambda_{rad} \ \text{(W/(m·K)} \qquad (2.1)$$

where λ_{tot}, λ_{gas}, λ_{solid} and λ_{rad} [W/(m·K)] are the total conductivity, the conductivity for gas conduction, the conductivity for solid conduction and the conductivity for radiation. Most commonly, the largest of these factors is the solid conduction. Therefore insulation materials are highly porous with small amount of solid structure.

In a material with a small amount of solid, the importance of the radiation will increase, as shown in Figure 2.1. This creates an optimal point from insulation perspective, for a certain material, where the sum of the contributions from radiation and solid conduction is at a minimum. This sum will add to the gas conduction which for conventional insulation materials can be considered as constant. This gives a total thermal conduction down to a minimum around 30 mW/(m·K), which can be compared to the air conductivity of 25 mW/(m·K). Figure 2.1 also shows the strong correlation between density and conductivity.

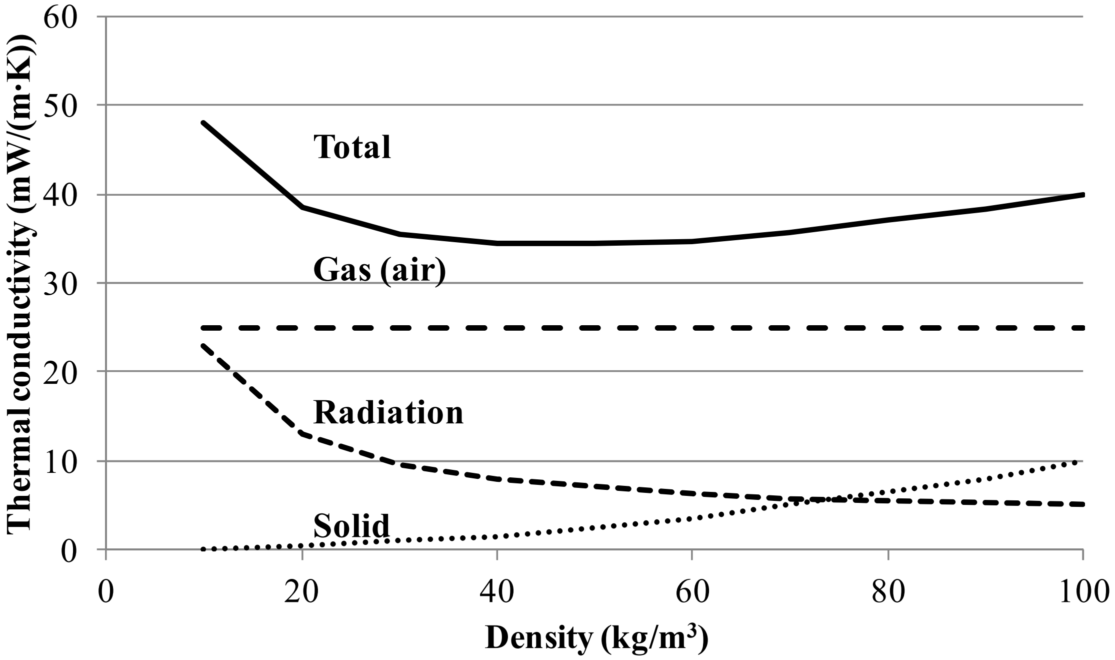

Figure 2.1. Thermal conductivity in porous materials divided in conduction through the solid, conduction through gas phase and radiation through pores (From Simmler et al., 2005).

Typical materials in this category are mineral wool, expanded or extruded polystyrene, loose-fill cellulose fibre or foam glass. Their thermal conductivities are presented in Table 2.1.

Table 2.1. Thermal conductivity of a number of common porous insulation materials (Peterson, 2007).

Insulation material	**Thermal conductivity, λ [mW/(m·K)]**
Mineral wool	33-40
Expanded/extruded polystyrene	30-40
Loose-fill cellulose fibre	39-42
Foam glass	39-45

2.1 Solid conduction

There is also some difference in the solid conduction for various materials. This makes the solid material and its physical properties important for the solid conduction. To minimize the solid conduction a proper solid material should be chosen.

As shown in Figure 2.1, the solid conduction will be decreased if the density is decreased. The actual conductivity in the solid will not change but the area of the solid in a cross section of the material will decrease, and thereby lower the solid conduction per square meter of the porous material.

As mentioned earlier, a decreased density will increase the heat flow due to radiation which will counter the gain in the solid conduction.

2.2 Radiation

Heat transfer by radiation is caused by the electromagnetic radiation which is emitted by all surfaces. The net radiation is the difference between the radiation from the warm surface and the radiation from the cold surface. The rate of heat transfer by radiation is dependent on the temperature of a surface which can be described by Equation (2.2).

$$\lambda_r = \frac{16n^2\sigma T^3}{3K} \quad \text{(W/(m·K))} \qquad (2.2)$$

where n [-] is the refraction index, σ [J/(K^4·m^2·s)] the Stefan-Boltzmann constant, T [K] the mean temperature and K [1/m] the extinction coefficient. With an increasing temperature, the heat transfer by radiation increases rapidly which can be counteracted by adding an opacifier to the material. Examples of opacifiers are titanium dioxide, TiO_2, which scatters the radiation or carbon soot which absorbs the radiation (Fricke et al, 1991). The additives will lower the conductivity but at the same time, the transparency of the material becomes lower.

2.3 Gas conduction

The gas conduction is based on the type of gas and the possibility for the gas to transfer heat. To get a lower value, the gas could either be exchanged to a gas with lower conductivity or by preventing the gas to transfer the heat. Examples of different gases and their thermal conductivity is shown in Figure 2.1 together with their molar weights.

Table 2.2. Thermal conductivity and molar weight of gasses (AGA, 1985).

Gas	**Thermal conductivity, λ [mW/(m·K)]**	**Molar weight [g]**
Air	25.5	29
Nitrogen, N_2	24.1 (0°C)	28
Argon, Ar	16.2 (0°C)	40
Carbon dioxide, CO_2	16.2 (25°C)	44
R-11, $CFCl_3$	8.3 (30°C)	137

A common solution where the gas is exchanged, is in windows where argon or krypton is used between the glazing panes. Another example is in polyurethane foam where reaction gases with low conductivity are trapped in a closed pore system.

The gas conductivity can be decreased by decreasing the pore size of the material. The collisions between the gas molecules and the solid are elastic which transfer small amounts of energy compared to the collisions between gas molecules. Smaller pores lead to a higher probability of collisions with pore walls instead of other gas molecules. This is called the Knudsen effect where the gas conductivity, λ_g, is governed by Equation (2.3) based on the Knudsen number, K_n [-], calculated by Equation (2.4) (Baetens et al, 2011).

$$\lambda_g = \frac{\lambda_{g0}}{1+2\beta K_n} \quad \text{(W/(m·K))} \tag{2.3}$$

$$K_n = \frac{l_{mean}}{\delta} \quad \text{(-)} \tag{2.4}$$

where δ [m] is the characteristic system size, which can be interpreted as the distance between two parallel walls, l_{mean} [m] is the mean free path, λ_{g0} [W/(m·K)] is the conductivity of the gas when moving freely and β [-] is a constant for the effectiveness of the energy transfer between the gas molecules and the solid pore walls with a value commonly between 1.5 and 2 (Baetens et al, 2011).

The gas conductivity is strongly dependent on the ratio between the pore size and the mean free path of the gas inside of the pores. The mean free path, l_{mean}, is the average distance a molecule travels before colliding with another molecule. The distance can be calculated by Equation (2.5).

$$l_{mean} = \frac{k_B T}{\sqrt{2}\cdot\sigma\cdot P_g} \quad \text{(m)} \tag{2.5}$$

where T [K] is the temperature, P_g [Pa] is the pressure, σ [m] is the molecular cross-sectional area and k_B [$1.38\cdot10^{-23}$ J/K] is the Boltzmann constant. For nitrogen and oxygen ,the main components of air, the molecular cross-sectional area is around 0.4 nm^2 (Engel and Reid, 2006). The mean free path for becomes approximately 70 nm at normal temperature and pressure (20°C and 100 kPa). The effect on the conductivity is shown in Figure 2.2.

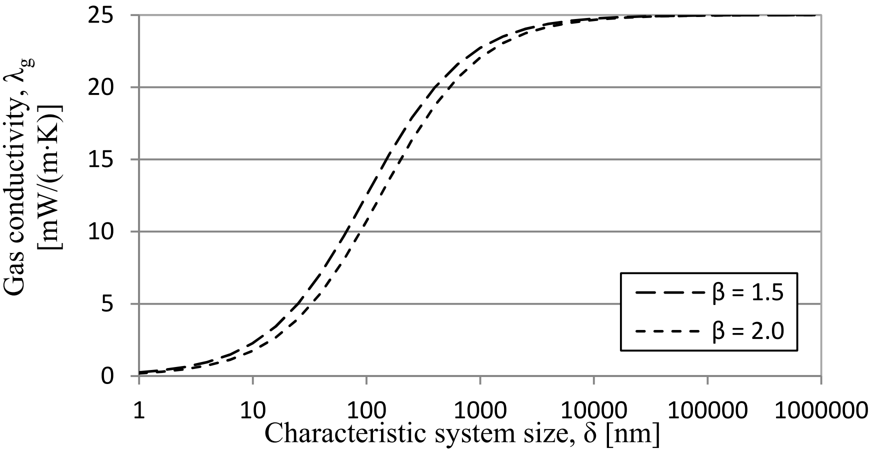

Figure 2.2. Calculated gas conductivity for air as a function of characteristic system size based on Equations (2.3), Equation (2.4) and Equation (2.5). The input temperature is 20°C and the pressure is 100 kPa. The characteristic system size can be related to the pore size of a material.

The characteristic system size can be difficult to determine but it is correlated to the pore size. However, when the pores grow larger, the conductivity get close to the normal conductivity of the gas. It seem as the Knudsen effect is negligible for pores larger than 10000 nm or 0.01 mm.

The effect on thermal conductivity, from a lowered pressure is strongly dependent of pore size. In Equation (2.5), pressure is seen in the denominator for the calculation of the mean free path. A lower pressure gives a longer mean free path which gives a larger Knudsen effect. From Equation (2.3) and Equation (2.4) it is seen that an increase in the mean free path will increase the Knudsen number and thereby decrease the gas conductivity. The effect on conductivity by changes in pressure is shown in Figure 2.3.

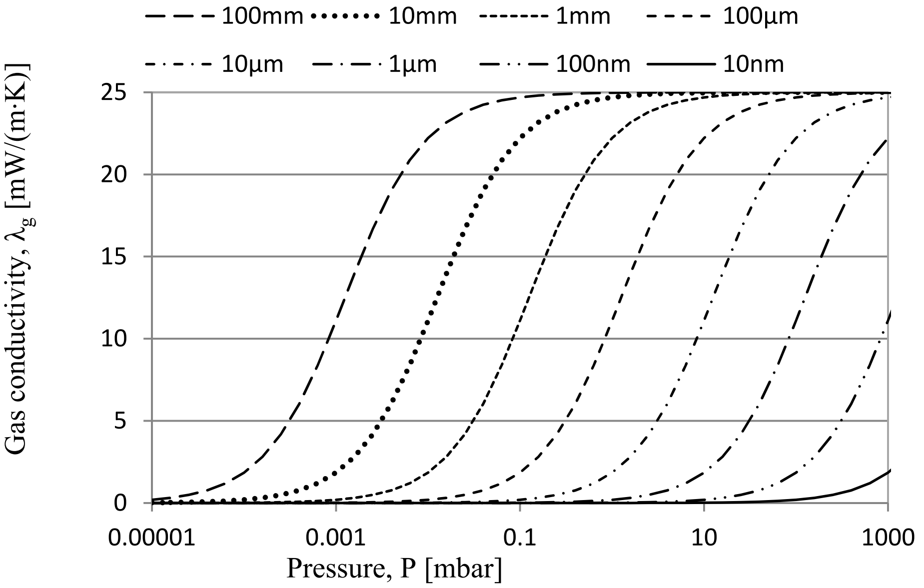

Figure 2.3. Calculated gas conductivity for air as a function of gas pressure for different characteristic system size based on Equations (2.3), Equation (2.4) and Equation (2.5). The input temperature is 20°C.

2.4 Convection in porous materials

Convection in porous materials can be separated in two cases, the convection inside the pore cells and the convection through the material on a macro scale.

For closed pore systems, such as EPS, there is no macro scale convection and for small pores, the pore cell convection can be neglected, partly because of small temperature differences on the cell walls. That means that the heat transfer through convection often can be neglected for materials with a closed pore system. For materials with open cells, the macro scale convection might have a considerable effect and can thus not be neglected.

The macro scale convection is either caused by natural or forced convection. For natural convection the air movement is created by density differences as a consequence of temperature differences, while forced convection is created by a pressure difference due to e.g. wind or fan induced.

Natural convection is described by the dimensionless quantity Nusselt number, shown in Equation (2.6), which is a function of the modified Rayleigh number, shown in Equation (2.7). The relation between the Nusselt number and the Rayleigh number is commonly determined empirically for specific geometries and boundary conditions.

$$Ra_m = \frac{\rho_a \cdot c_{pa} \cdot g \cdot \beta_a \cdot d \cdot k \cdot \left(T^+ - T^-\right)}{\nu \cdot \lambda_m} \quad (\text{-}) \tag{2.6}$$

$$Nu = \frac{q_{\text{with convection}}}{q_{\text{without convection}}} \quad (\text{-}) \tag{2.7}$$

where ρ_a [kg/m^3] is the density of air, c_{pa} [J/(kg·K)] is the specific heat capacity of air, g [m/s^2] is the gravitational acceleration, β_a [1/K] is the thermal expansion coefficient of air, d [m] is the thickness of the porous material, k [m^2] is the permeability, T^+ and T^- are the temperatures on the warm and the cold side respectively, ν [m^2/s] is the kinematic viscosity, λ_m [W/(m·K)] is the thermal conductivity of the porous material and q [W/m^2] is the heat flux through the material.

The air flow through a layer of a porous material due to forced convection can be calculated by Equation (2.8). The pressure difference can for example be created either by wind or by a fan.

$$\dot{V} = A \frac{k}{\mu} \frac{\Delta P}{d} \quad (\text{m}^3/\text{s}) \tag{2.8}$$

where A [m^2] is the area, k [m^2] is the permeability, μ [kg/(m·s)] is the dynamic viscosity and d [m] is the insulation thickness.

The material properties relevant for convection are the permeability, both for natural and forced convection, and the thermal conductivity which only affects the natural convection.

3 Aerogel

An aerogel is a former gel from which the liquid phase has dried out. To be an aerogel, as opposed to a xerogel, the solid structure in the gel has to be preserved throughout the drying (Iler, 1979).

The concept of aerogels were first investigated by Kistler (1931a) in the early thirties. Kistler's hypothesis was that the shrinkage was created by capillary forces during the drying. To test the hypothesis Kistler heated his gel samples to the critical temperature of the liquid while the pressure was held above the vapour pressure of the liquid. Above the critical temperature, the liquid's transition into gas will not subject the gel structure to tension, which leaves a dry gel with the structure intact. The experiments were successfully tested for a wide variety of gels (Kistler, 1931b).

Most commonly used for building applications are silica aerogels which are formed from a silicon based gel. These are transparent aerogels with high porosity and pores with an average diameter in the range between 20-40 nm (Soleimani Dorcheh et al., 2008). Due to the Knudsen effect, explained in Section 2.3, the thermal conductivity can become lower than for still air (< 25 mW/(m·K)).

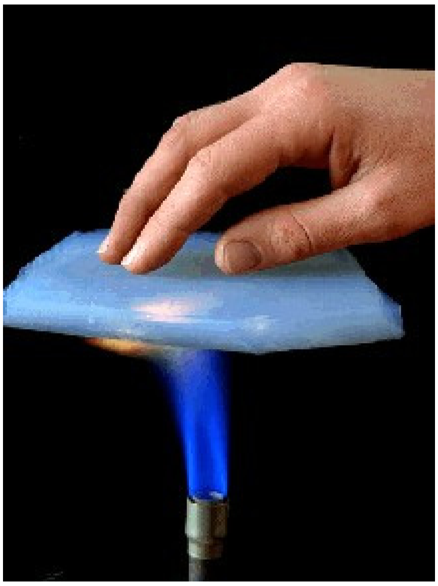

Figure 3.1. Photo of an aerogel above a blow torch. (Photo: Aerogel, 2012).

The aerogel can be produced as monolithic blocks, as granulates of varying fineness or as carpets reinforced by some fibre material. There are also a variety of aerogel composites.

3.1 Properties

Monolithic silica aerogel is a brittle material. Parmenter and Milstein (1998) measured the compressive strength to around 1 MPa while the tensile strength and the shear strength were much lower.

Silica aerogels has commonly a density around 100 kg/m^3 (Soleimani Dorcheh et al., 2008) but Tillotson et al. (1992) managed to prepare samples with as low density as 3 kg/m^3 which is only 2.5 times the density of air, 1.2 kg/m^3. Even though it has a very small amount of solid material it has also very small pores with a diameter in the range of 20-40 nm. It is the combination of small pores and a small fraction of solid that leads to the good thermal performance of the aerogel.

For thermal properties of aerogel, there are two different positions from which to optimize the performance. Aerogels can be transparent to a certain degree and thus be used as a light inlet with very low thermal conductivity compared to glass. At the same time this will mean a relatively large conductivity from radiation. The aim could also be to optimize the thermal properties and thus try to minimize radiation through the material.

3.1.1 Transparent aerogels

Silica aerogels are commonly transparent. An example of transparent aerogel granulates are shown in Figure 3.2.

Figure 3.2. Granulates of transparent silica aerogel (Photo: Axel Berge).

Rubin et al (1982) investigated the optical and thermal properties of aerogel windows. A transparent aerogel with a conductivity of 19 mW/(m·K) was tested. Because of the brittleness of monolithic aerogel, the aerogel was fitted between two glass panes for protection. For common window glass, an 8 mm thick aerogel layer had a transmittance of 0.6, which is similar to the transparency of a triple glass window. By exchanging the protective glass to one with lower iron content, the thickness could be increased to 14 mm keeping a transmittance of 0.6. For an aerogel layer of 6 mm the transmittance could be enhanced to 0.7, similar to a double glass window. Rubin et al (1982) found the 6 mm aerogel window to have an U-value of around 2 W/(m^2·K) and a 14 mm thick aerogel window got a U-value close to 1 W/(m^2·K).

Nilsson et al (1985) reached a conductivity of 17 mW/(m·K) for a transparent aerogel. The measurements were made by the hot strip method. The heat source in the hot strip method has a very low emissivity which would yield low heat transfer from radiation. In other words the transparent aerogels might let out indoor heat radiating from interior surfaces. The effect of radiation through an aerogel sample was measured by Sheuerpflug et al (1985). The conductivity in evacuated aerogel was measured with a guarded hot plate apparatus. Between the measurements the surface in contact with the aerogel was exchanged between materials with varying emissivity. The measurements showed that the boundaries of the aerogel had an impact on the measured conductivity, which led to a formula for a pseudo-conductivity which is dependent of the specimen thickness. For a 10 mm thick evacuated aerogel tile in a low emissivity envelope, the apparent conductivity was measured to around 10 mW/(m·K).

Caps et al (1984) quantified the radiative conductivity and found it to be around 2 mW/(m·K) at room temperature. For higher temperature applications the radiative conductivity would get an increased importance. Reim et al (2004) concludes that silica aerogel commonly has a very low extinction coefficient for electromagnetic waves with a wave length below 7 µm. At room temperature most of the heat radiates above this limit but for higher temperatures a larger proportion of the radiated heat will transmit through the aerogel. The Rosseland mean extinction peaks around 50°C with 0.14 m^2/g and decrease to around a third at 350°C.

3.1.2 Opacified aerogels

With some kind of opacifying agent, the radiatiative conduction in the aerogel can be reduced. Fricke et al (1991) made conductivity measurements for monolithic silica aerogels with various densities and amount of added soot. Their lowest recorded thermal conductivity was 13 mW/(m·K) at room temperature. It was achieved for an aerogel sample with a density of 120 kg/m^3 and 5% soot content.

Fricke et al (1991) also found that both the solid conductivity and the gas conductivity was proportional to the density with the relation shown in Equation (3.1) and Equation (3.2). Hümmer et al (1993) used these relations and an equation for the radiative conductivity to come up with Equation (3.3), which is a relative equation for the thermal conductivity of opacified silica aerogels.

$$\lambda_{gas} \propto \rho^{-0.6} \tag{3.1}$$

$$\lambda_{solid} \propto \rho^{1.5} \tag{3.2}$$

$$\lambda_{tot}(\rho) = \lambda_{solid,0}\left(\frac{\rho}{\rho_0}\right)^{1.5} + \lambda_{gas,0}\left(\frac{\rho}{\rho_0}\right)^{-0.6} + \lambda_{rad,0}\left(\frac{\rho}{\rho_0}\right)^{-1}\left(\frac{T}{T_0}\right)^{3} \tag{3.3}$$

where ρ [kg/m^3] is the density, λ_{tot}, λ_{gas}, λ_{solid} and λ_{rad} [W/(m·K)] are the total conductivity, the conductivity for gas conduction, the conductivity for solid conduction and the radiative conductivity, T [K] is the temperature and the index 0 means that the parameters are related to a reference material.

From an aerogel, where the separated conductivities through radiation, solid, gas and the density is known, Equation (3.3) can be used to calculate the conductivity of any new aerogel of the same type. At room temperature, the function shows a minimum value around a density of 100 kg/m^3.

Hümmer et al (1993) studied the thermal conductivity for opacified aerogel ground to granulates or powder. Ground aerogels could be used as filling in complex geometries. Both the granular and powder aerogels showed higher conductivity than monolithic aerogel at ambient pressure, above 20 mW/(m·K), but for lower pressures the conductivity of powder aerogel decreased below that of monolithic aerogel. For a powder aerogel, optimized for low evacuated conductivity, Hümmer et al (1993) reached down to 1.8 mW/(m·K) when the pressure was 1 Pa.

To handle the brittleness of aerogel, it could be reinforced by some kind of fibrous material. Stepanian et al (2006) have a US patent on aerogels gelated in a lofty batting. The reinforced aerogels form carpets with very small amounts of solid. In their patent application, they presented tests where they had reached conductivities close to 10 mW/(m·K) at room temperature. The carpets are flexible and the shear and tensile strength of the aerogel are greatly enhanced. An aerogel carpet is shown in Figure 3.3.

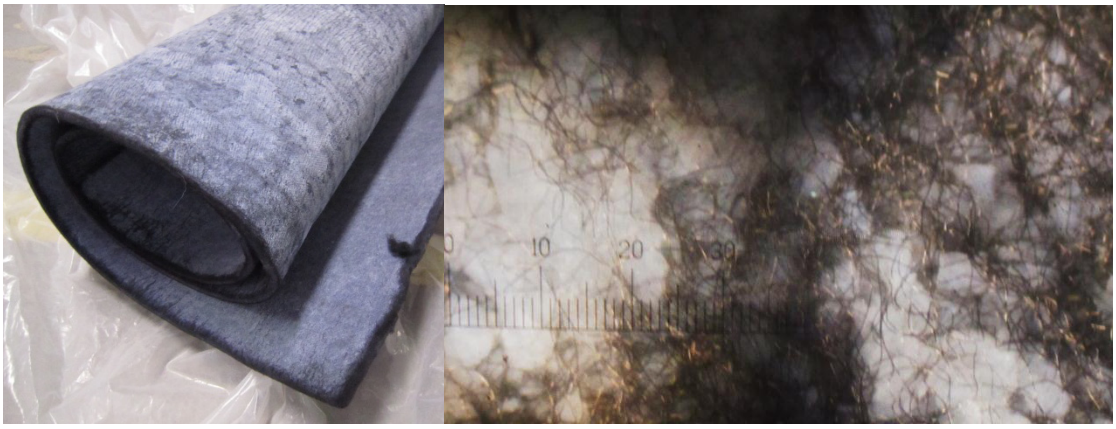

Figure 3.3. Aerogel blanket, a 1x1m sheet to the left and a magnified image of the surface to the right (Photo: Axel Berge).

3.2 Production

The first step in producing an aerogel is to produce the gel. The gel is commonly produced in a sol-gel process, where the solid components of the gel are dispersed in a solvent such as water or alcohol. Gelation occurs and the gel is formed with the solvent dispersed as liquid in the gel pores.

During normal drying of a gel, parts of the solid structure will collapse due to the pressure created when the liquid in the pores evaporate. This leads to a significant shrinkage of the gel, and consequently the density of the solid gets higher. To minimize the shrinkage, the gel can be dried at the liquids critical state, above its critical temperature and critical pressure.

Above the critical state, the liquid becomes a supercritical fluid. There is no longer any difference between its liquid state and its gas state and there will not be any tension created by the phase change. In this way, the solvent can be dried out without affecting the structure of the solid, thus leaving a highly porous low density material, an aerogel (Kistler, 1931b).

The process can be illustrated in a phase diagram as in Figure 3.4. The figure shows the temperature and pressure related to the different phases of the pore liquid. The liquid starts at ambient conditions (point 1.) and the temperature and pressure are continuously raised until the supercritical state is reached (point 2.). The combination of pressure and temperature is constantly held above the line for the conditions separating the liquid phase from the gas phase (e.g. following the dashed arrow). This way, the fluid will stay as a liquid until the critical state is reached where it can be exchanged with another fluid, most commonly air, without creating any forces on the gel structure.

After the fluid exchange, the temperature and pressure can be reduced to ambient conditions again without impact on the gel structure. Left is a dried gel with the original gel structure intact.

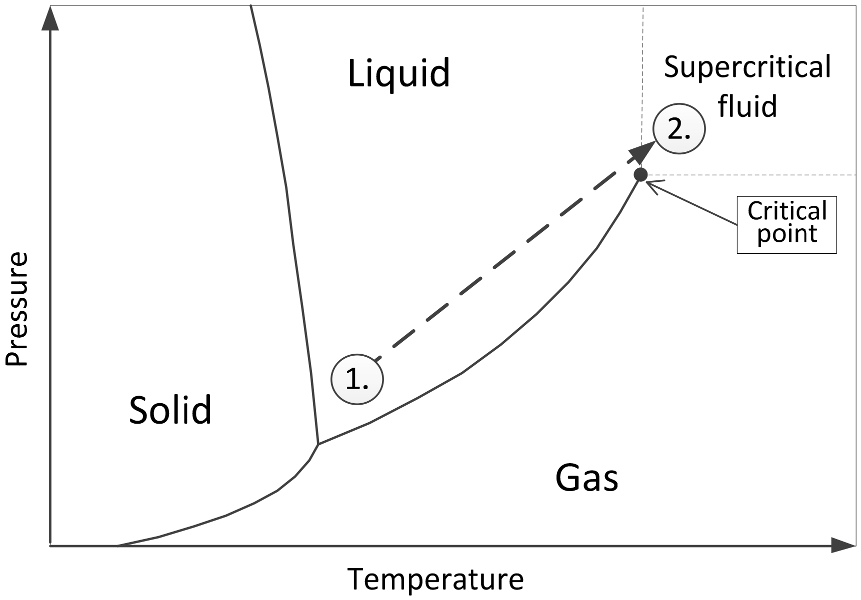

Figure 3.4. Example of a phase diagram.

For water the critical temperature and pressure are 374°C and 221 bar respectively. This means that a high pressure and high temperature are needed to create an aerogel from a gel with water as the fluid. To decrease the energy needed to create aerogel, the liquid in the gel can be exchanged to a liquid with a lower critical temperature and/or critical pressure. In Table 3.1 some different liquids are compared. Especially carbon dioxide is interesting since its critical temperature is 31°C which is very close to normal room temperature. But for most fluids, the critical pressure is large compared to atmospheric pressure. This means that production of aerogel has to be energy intense.

Table 3.1. Some different fluids and their critical temperature and critical pressure (NIST, 2011).

Fluid	**T_{cr} [K]**	**T_{cr} [°C]**	**P_{cr} [bar]**
Water, H_2O	647 ± 2	374 ± 2	221
Methanol, CH_3OH	513 ± 1	240 ± 1	81 ± 1
Carbon dioxide, CO_2	304	31	74

Dowson et al (2011) made a life cycle assessment of transparent silica aerogel. They did not have numbers from actual industrial made products, so they evaluated the process of laboratory produced aerogel. Their assumption was that an industrial production would lower the environmental impact even further since the aerogel would be produced in larger batches. They calculated a refurbish example where single glazing windows were replaced with transparent aerogel. The energy savings were larger than the energy used in production after 0.3 to 1.9 years. A comparison with single glazed windows might be somewhat misleading since the solar transmission will decrease, as discussed in Section 3.1.1, and there are better refurbishing alternatives with double or triple glazed windows.

Kirkbir et al. (1998) dried silica aerogel at various pressures between atmospheric and critical pressure for some different liquids. The hypothesis was that there is a threshold pressure above which the forces created in the pores during drying are weaker than the strength of the gel structure. They found that for some solvents the critical pressure could be more than halved without cracking of the aerogel and with shrinkage of only 2 percent. This still required a pressure of 18 bar.

There is a method for drying of aerogels at ambient pressure where the gel is prepared by silylation, a substitution of silyl groups to the gel structure. The silylation makes the gel highly hydrophobic which decrase the forces from the evaporation of the cell water. At a first stage, the gel shrinks due to internal water flows but when enough water has left, the remaining water will form droplets inside the cell structure which will repel the pore walls and the solid structure will spring back towards its original size (Soleimani Dorcheh et al., 2008). Parvathy Rao et al. (2005) measured the thermal conductivity of aerogel samples dried at ambient pressure and reached down to around 100 mW/(m·K) which is far above the properties of aerogels dried at supercritical condition.

3.3 Applications

As mentioned in Section 3.1.1, aerogels can be used in energy efficient windows. However, the U-values found by Rubin et al (1982) is not better than those of modern triple glazed windows. The U-value could be enhanced by evacuating the aerogel which was done by Caps and Fricke (1984) who got a U-value around 0.7 W/(m^2·K) for 1 cm thick aerogel and 0.35 W/(m^2·K) for 2 cm thickness. They did not report any value for the solar transmission.

Another investigated use of transparent aerogel is as a solar collector. Schreiber et al (1986) explored the effects of mounting a transparent aerogel insulation layer on the outside of the external walls. The solar radiation will transmit through the aerogel and heat the wall behind. If the conductivity of the wall is high compared to the aerogel, the energy from the solar radiation will flow into the building. With a heavy internal wall the heat could also be stored.

Svendsen (1992) moulded transparent aerogel around a metal solar collector connected to water pipes. For a 60°C system, the annual energy gain per square meter of the solar collector reached 766 kWh compared to 316 kWh for a typical solar collector without aerogel. For an 80°C system the annual energy gain per square meter solar collector was 684 kWh with aerogel and 183kWh without aerogel.

Opaque aerogels could be used as insulation in the building envelope to decrease the wall thickness. Today it is very expensive with more than ten times the cost of common insulation materials such as mineral wool (Baetens et al, 2010).

Reinforced aerogel carpets are used as pipe insulation (Baetens et al, 2010). With a lower conductivity, the pipes can be made smaller which is beneficial for transport and space needed for installation. For pipes the thickness is of large importance since the heat losses are radial. The insulating capacity has a greater importance the closer it is to the center of the cylinder where the circumferring area is smaller. A halving of the thermal conductivity would give more than half the insulation thickness for the same design losses.

Stahl et al (2012) blended aerogel into a façade rendering. The rendering reached a conductivity of 25 mW/(m·K) which is lower than conventional rendering systems. The density was 200 kg/m^3. The rendering is still under development but could be a good alternative for exterior insulation when refurbishing old buildings.

4 Vacuum insulation panels (VIP)

Vacuum insulation panels (VIP) consists of a core material with small pores, around 10-100 nm, which is enclosed in a thin laminate film with low gas permeability. The core material is evacuated to pressures of 0.2-3 mbar which, depending on core material, give a thermal conductivity of 2-4 mW/(m·K). The laminate is not perfectly gas tight which makes it possible for gas molecules to diffuse through the envelope which leads to an irreversible pressure increase in the VIP. The speed of the pressure increase is dependent on core material, type of laminate and the surrounding climate (Simmler et al., 2005). This review is based on the available literature where most studies have been performed on VIP with a fumed silica core with a metalized multi-layered laminate. Other products exist but are not as well described in the literature.

The first patent of VIP is from 1930 when a German patent on a rubber enclosed porous body was filed. Twenty years later a patent on a glass wool core welded to a steel foil was filed in the US. In 1963, the first patent of a panel with a core of a nanostructured material was filed. The development of VIP continued with experiments of different core material and envelope techniques. The increasing demands from food, pharmaceutical and electronic industries boosted the development of thin laminates with low permeability. Nanostructured materials that could be used in the core were available already in the 1930s following Kistlers experiments with aerogels. However, the commercial production of aerogels was suspended in the 1970s which lead to development of alternative core materials (Fricke et al., 2008).

Figure 4.1 shows a VIP of the type that is common today (June 2012) which was first introduced in the early 1990s. The core material was at that time precipitated silica which was enclosed by a plastic envelope with a 12 µm thick aluminum film. Another product that was introduced at the same time was a VIP with a fiber core and an envelope of 75 µm thin welded sheet steel. The product was intended for the refrigerator industry and the thermal conductivity of the products ranged around 2-7 mW/(m·K). A VIP with a diatomite[1] filling and a 100 µm sheet steel casing was also tested for application in district heating pipes. The thermal conductivity for the diatomite VIP was around 5-10 mW/(m·K). In 1998, the first application of VIP in a building was reported from ZAE Bayern where a test façade was insulated with VIP (Fricke et al., 2008).

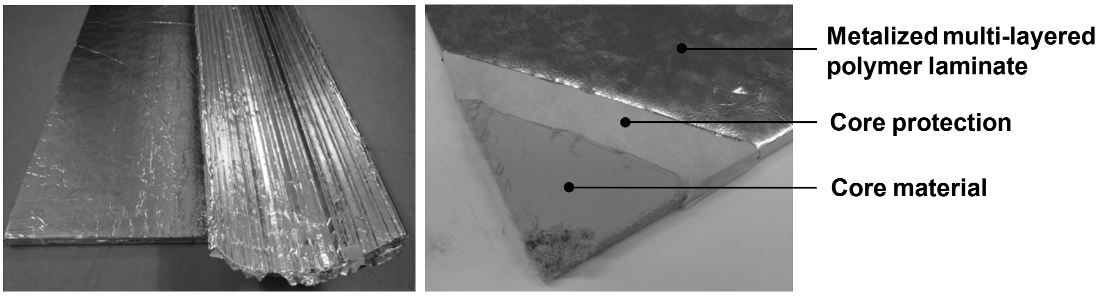

Figure 4.1. Flat and folded VIP with the core material, protection layer and heat sealed metalized multi-layered polymer laminate (Photo: Axel Berge).

---

[1] Sedimentary rock which is composed of 80 to 90% silica, 2 to 4% alumina and 0.5 to 2% iron oxide. The thermal conductivity is 0.06 W/(m·K) and the density is 400 kg/m^3.

Three Swiss life cycle analysis (LCA) methods were used by Schonhardt et al. (2003) to study the environmental impact by VIP with fumed silica wrapped in a metalized multi-layered laminate film. The VIP was compared to the equivalent amount of glass wool and expanded polystyrene (EPS) used in 1 m^2 wall with a U-value of 0.15 W/(m^{2}K). The first method measures the embodied energy (MJ/m^2) which is a summation of how much energy that has been used in the production and processing of the material. The second method was the UBP97 method which makes it possible to compare materials in regard of resource use, production of radioactive waste, need of landfill and emissions to air, water and ground. The third method is called Eco-indicator 99 (Eco99) and is used to calculate the impact by production on the human health, effects on the eco system and resource depletion. The method uses a weighting system where the impact on different time scales, e.g. impact on future generations, is taken into account. Also the environmental impact on local and global scale is included in the model. Table 4.1 presents the results of the three methods with the absolute values and as percentage of the results for VIP. A comparison between aerogel and VIP should be interesting but since no LCA of the aerogel materials could be found it was not possible here.

Table 4.1. Results from three different Swiss LCA methods for 1 m^2 material with a U-value of 0.15 W/(m^{2}K) where the equivalent amount of glass wool and EPS are compared to VIP (Schonhardt et al., 2003).

Method	Glass wool		EPS		VIP	
	Abs.	% of VIP	Abs.	% of VIP	Abs.	% of VIP
Embodied energy (MJ/m^2)	455	46	890	89	999	100
UBP97 (UBP97/m^2)	21 646	50	35 767	83	43 245	100
Eco99 (milli-points/m^2)	1 254	52	3 402	142	2 393	100

The LCA calculations showed that the VIP is worse than glass wool and EPS in regard of embodied energy and UBP97 methods. Eco99 showed that VIP had a lower environmental impact than EPS which was 42% higher than VIP, while mineral wool was only half compared to VIP. The high figure for EPS was caused by the use of fossil based goods. The analysis showed that 90% of the energy used in VIP production derived from the core material while only 4% was used for the laminate production. With an alternative core material or a more energy efficient process, calculations show that the environmental impact of VIP could be lowered by 45% (Schonhardt et al., 2003).

4.1 Envelope

Today the most common VIP envelope is a metalized multi-layered polymer laminate which is heat sealed to form a continuous envelope. Examples of different layers and thicknesses of the laminate are presented in Figure 4.2.

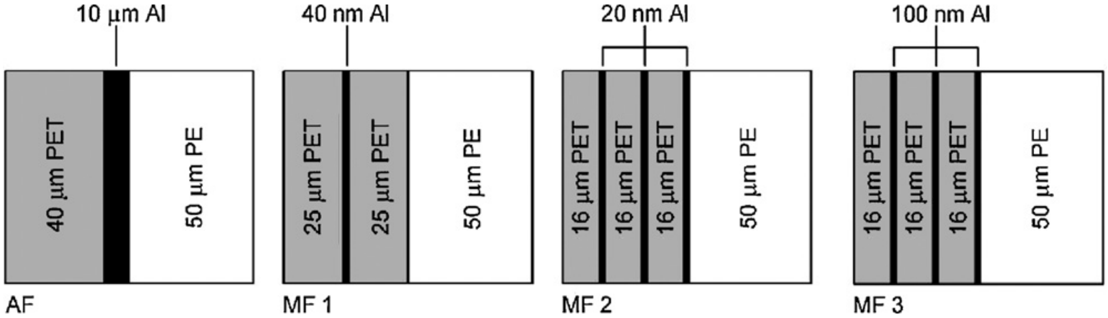

Figure 4.2. Metalized multi-layered polymer laminates are used to encapsulate the core material of the VIP. The laminates are manufactured by adding layers of varying thickness and material (Willems et al., 2005).

The pressure inside the VIP should not increase above 100 mbar within 30-50 years since the thermal conductivity of the core material increases rapidly at higher pressure, as shown in Figure 4.4. To reach this value, the oxygen transmission rate (OTR) of the envelope has to be below 0.01 $cm^3/(m^2day)$ at 1 bar pressure difference. The water vapor transmission rate (WVTR) of the envelope has to be below 10^{-4} $g/(m^2day)$ under specific conditions of temperature and humidity at each surface. The low transmission rates make it very difficult to measure the properties of the laminate. Brunner et al. (2008) measured the pressure increase of different VIP samples, size 25x25x2 cm and 50x50x2 cm, in 23°C and 50% relative humidity on the outside and 5% on the inside. For a metalized multi-layered laminate, the OTR was around 0.001-0.002 $cm^3/(m^2day)$. The WVTR was 0.003-0.005 $g/(m^2day)$ with a water vapor partial pressure difference of 14 mbar between the outside and inside. Garnier et al. (2011) studied the influence of varying the number of metalized layers and the thickness of the aluminum coating. Experimental results showed that the WVTR decreased exponentially with the thickness of the aluminum while the number of metalized polymer layers had smaller effect on the permeability.

A very important factor influencing the service life of the VIP is the durability of the laminate over time. Brunner et al. (2008) studied the influence by moisture and elevated temperature experimentally. A number of VIP were stored in 65°C and 75% relative humidity during 1 year which is an extreme climate compared to the actual climate in a building. After 100 days, the laminate was mechanically deformed and beginning to delaminate but still functioning. Within a year, the laminate failed and the VIP was filled to ambient pressure. In another experiment, VIP were stored in 80°C and 80% relative humidity for 8 hours and then the climate was changed to 25°C and 50% relative humidity for 4 hours. The result was that the aluminum oxidized and transparent spots where visible on the panels after 26 days (Brunner et al., 2008).

Garnier et al. (2011) identified a number of factors that influence the durability of the aluminum layers in the laminate. Experiments on different glues in the laminate were performed to identify harmful combinations. The aluminum oxide was not stable in acidic (pH<4) or alkaline (pH>9) environments. Fluoride ions, which are present in drinking water, were identified as one of the chemical compounds that could cause degradation of the laminate. To produce durable laminates, the glue should be free of chlorides and other substances such as Ga, Tl, In, Sn, Pb which also could reduce the stability of the aluminum in the laminate.

The multi-layered polymer laminate is highly flammable and will start decomposing at around 150°C causing production of carbon monoxide, formaldehyde and possibly other aldehydes. The laminate auto ignites at around 350°C (Microtherm, 2009) with a fast fire development, see Figure 4.3. Newly developed VIP has a 6 µm thick flame-retardant brominated acrylic copolymer coating on the outside of the laminate. In Germany, the VIP is classed according to DIN 4108-10 as B2 which is the same class as for wood and other materials with normal combustibility (Porextherm, 2009).

Figure 4.3. Melting and burning of a metalized multi-layered polymer laminate film (Photo: Bijan Adl-Zarrabi).

4.2 Core material

The core material most commonly used on the European market is fumed silica, SiO_2, which is produced from silicon tetrachloride, $SiCl_4$, by pyrolysis. Silicon tetrachloride is used in semiconductor industry and in the production of photovoltaic cells. Other materials used in the core are glass wool, polyurethane and polystyrene. The thermal resistance of a material depends on the thermal conductivity of the solid material, convection and gas conductivity in the pores and radiation between the surfaces of the pores as discussed in Chapter 2. Figure 4.4 shows the relation between the ambient pressure and the thermal conductivity of a number of different materials common in the VIP core.

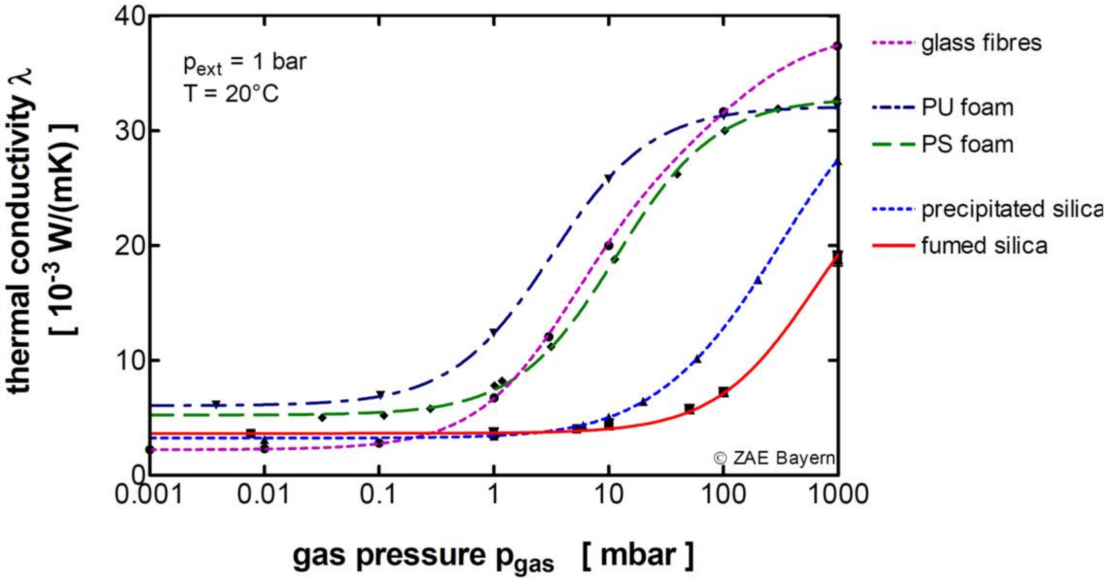

Figure 4.4. Thermal conductivity of different materials which are used in the core of VIP as a function of the ambient pressure. Normal atmospheric pressure is 1 000 mbar (Simmler et al., 2005).

Three distinct areas are visible in Figure 4.4 which are governed by the three modes of heat transfer through the material. The glass wool is a porous material with large cavities where the heat transfer by convection and gas conduction are dominant at atmospheric pressure. Polystyrene, polyurethane and precipitated silica have smaller pores compared to glass wool which means that the gas conduction and convection are smaller in these materials. The pore size of fumed silica is around 10-100 nm which is the same order of magnitude as the mean free path of air molecules, around 70 nm, in normal temperature and atmospheric pressure. When the pressure decreases towards vacuum, the heat transfer by gas conduction and convection decreases and heat transfer by radiation and conduction through the solid are left. They are constant as long as the temperature and density of the material are left unchanged.

The density of fumed silica is, depending on producer, around 160-190 kg/m^3 which is significantly higher compared to e.g. glass wool 20-80 kg/m^3 and polyurethane foam 30 kg/m^3. Measurements of the porosity of the fumed silica have shown that it is also very high, above 90%. The high porosity means that fumed silica has a very high specific surface area which is important for the hygroscopic moisture properties. Hardened cement paste has a specific surface area of around 150 m^2/g which is similar to fumed silica with around 200 m^2/g. The specific heat capacity of fumed silica is around 850 kJ/(kg·K) (Simmler et al., 2005). Fumed silica is nonflammable and is therefore classified A1 according to DIN ISO EN 13501-1 (Porextherm, 2009).

The pressure in the VIP is reduced to an initial internal pressure of 0.2-3 mbar during production. Glass wool has the lowest thermal conductivity of the common core materials below 0.1 mbar. However, the thermal conductivity increases fast with an increasing pressure which gives a short service life of the VIP. Also glass wool emits gases when it is aging which leads to an irreversible pressure increase in the VIP. A getter, e.g. barium, can be used in the core to absorb the gases, maintaining the low pressure in the core and prolonging the service life. The influence of moisture uptake in the panel during operation can be reduced by adding a desiccant to the core of the VIP. No getter is needed when using fumed silica in VIP since it is a stable material. Fumed silica also works as a desiccant with a moisture content of around 0.016 kg/kg at 30% relative humidity, 0.067 kg/kg at 75% and 0.195 kg/kg at 95% (Simmler et al., 2005). However, Morel et al. (2009) found that fumed silica exposed to a high relative humidity results in an increase in the moisture capacity. The consequence of this is that the specific surface area decreases leading to a higher thermal conductivity of the fumed silica.

The fumed silica is beneficial over the other materials since it has a lower thermal conductivity at higher internal pressure, which prolongs the service life of the VIP. Alternative core materials are being explored in order to find substitutes for the expensive fumed silica. Mukhopadhyaya et al. (2008) investigated the thermal conductivity of two layered composites under varying ambient pressure. The materials were produced from fibrous insulation boards which were mixed with pumice powder. The thermal conductivity at low pressure showed similar behavior as the fumed silica up to around 100 mbar, but was significantly higher at atmospheric pressure.

4.3 Thermal bridges

The metalized multi-layered laminate film around the VIP creates a thermal bridge as shown in Figure 4.5. A thermal bridge is defined as the linear thermal transmittance, ψ (W/(m·K)), which is multiplied with the length of the thermal bridge, i.e. the perimeter of the VIP. The magnitude of the thermal bridge is dependent on the center-of-panel thermal conductivity and the thermal conductivity of the laminate. Also the thickness of the panel and laminate influences the thermal bridge together with the air gaps between the panels and the thermal conductivity of the surrounding materials (Binz et al., 2005).

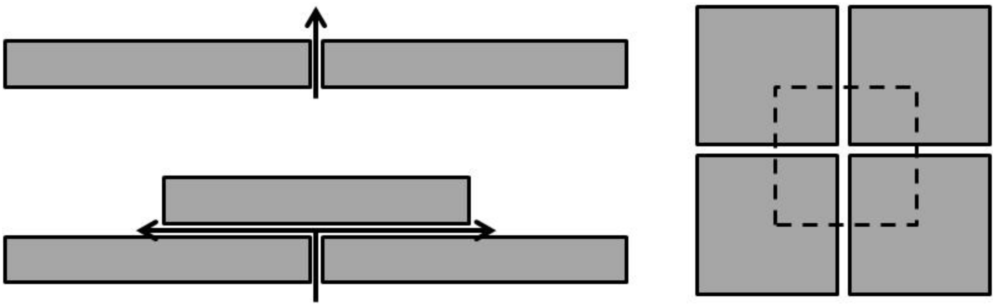

Figure 4.5. Thermal bridge around the perimeter of the VIP. The thermal bridge can be blocked by adding a second layer of VIP.

Studies of the thermal bridges created by the VIP envelope have been performed by a number of researchers. Schwab et al. (2005) used two dimensional finite differences to calculate the influence by air gaps between the VIP and also investigated the influence by encapsulating the VIP in polystyrene. The simulations showed that the effective U-value of a 500x500x20 mm large panel increased with up to 360% for the laminated aluminum film with a 5 mm air gap. The effective U-value for the VIP with metalized multi-layered polymer laminate film only increased with 44% with the same air gap. Brodt and Bart (1994) used finite differences to calculate the influence by the VIP laminate on the effective thermal conductivity of a VIP in a refrigerator. The VIP was coated with a 50 µm thick layer of aluminum which gave a high thermal bridge effect. With a metalized multi-layered polymer laminate, the effective thermal conductivity would be decreased by 50%.

Ghazi Wakili et al. (2004) compared two- and three dimensional numerical simulations with measurements of the thermal bridge effect of the laminate on 20 mm thick VIP of sizes 500x500 and 500x250 mm. The laminate was modeled layer by layer where each type of material in the laminate was put in one layer with the total thickness of the material. Two different laminates were tested, one laminate with a total aluminum thickness of 90 nm and another laminate with 300 nm. The measurements resulted in a 3-6% higher heat flow than what the simulations predicted. The higher deviation was found for the laminate with the thicker aluminum layer and the lower for the laminate with less aluminum. The linear thermal transmittance was 7 mW/(m·K) for the 90 nm aluminum and 9 mW/(m·K) for the 300 nm aluminum. The increased heat flow through the laminate leads to a higher effective thermal conductivity of the VIP; 14% higher for the laminate with 90 nm aluminum and 19% higher for the laminate with 300 nm aluminum compared to the centre-of-panel thermal conductivity.

In a follow-up study by Ghazi Wakili et al. (2011), the effect of the laminate in constructions with double layered VIP was investigated. Different arrangements of 15-40 mm thick, 500x500 and 500x250 mm panels were measured in guarded hot plate apparatus. The panels were encapsulated in a multi-layered polymer laminate with a total aluminum thickness of 300 nm. The panels had an average centre-of-panel thermal conductivity of 4.1 mW/(m·K). The average linear thermal transmittance was around 2.5 mW/(m·K) for the case with a layer of two small panels on top of an unbroken layer of VIP.

The measurements by Ghazi Wakili et al. (2011) were compared to a simplified numerical model where the laminate was treated as a 0.1 mm thick layer of the equivalent thermal conductivity and the core was treated as a homogenous material with a thermal conductivity of the measured centre-of-panel value. The results showed that the effective thermal conductivity of the laminate was approximately 20 times higher than what is the case using the weighted arithmetic mean of the conductivities of the layers in the laminate. The effective thermal conductivity is highly influenced by the width of the air gaps between the panels and on the properties of the surrounding materials which are not taken into account in the simplified numerical model. The mean value of the materials is in the area of 0.4-0.5 W/(m·K) while an equivalent thermal conductivity of the laminate of 10 W/(m·K) had to be used by Ghazi Wakili et al. (2011). This value is in the same order of magnitude as own measurements presented in Johansson (2012a). The weighted arithmetic mean was used by Grynning et al. (2011) who compared numerical simulations with hot box measurements of single and double layer VIP. The effect of the thermal bridges was larger in all their measurements compared to their corresponding numerical simulations, which might be explained by the higher effective thermal conductivity of the laminate.

4.4 Quality assurance

VIP is a material that easily can be damaged at the construction site. It can either be caused by lack of awareness of the construction workers or the VIP was already damaged when it left the production facility. The easiest way to detect a punctured panel is by visual detection. At a certain degree of inflation, the laminate gets lose and wrinkles. In-situ measurement of the thermal conductivity on the construction site is complicated with the techniques available today. Meanwhile, at the VIP production facility, the thermal conductivity of the finished VIP can be measured.

Since the core and laminate of the VIP have very different properties, direct measurement of the thermal properties is complicated. There exist indirect methods that measure the internal pressure of the panel, e.g. the foil lift-off method and integration of a pressure sensor in the VIP. The methods rely on the empiric relation between internal pressure and thermal conductivity that is used to evaluate the properties of the VIP. Erbenich (2009) described the available methods and concluded that it does not exist a method that can be used on the construction site to measure the thermal conductivity to ensure that the VIP has not been damaged after it left the production plant.

Caps (2005) described an indirect measurement method which could be integrated in the quality assurance process of the VIP production line. An integrated fiber material of known thermal conductivity at different pressures is placed between the VIP envelope and a heat sink, e.g. a metal plate, in the core material. The fiber material is installed since the thermal conductivity increases faster at increasing pressure than in the core material, see Figure 4.4. A heated sensor is placed on the surface of the panel, close to the heat sink, during a specified time period. The temperature decrease of the sensor is registered and with the known relation between the temperature decrease and thermal conductivity of the fiber material, the interior pressure of the VIP can be determined. The empiric relation between internal pressure and thermal conductivity is then used to derive the thermal conductivity of the VIP.

Johansson et al. (2012) investigated if the method by Caps (2005) could be refined and used without insertion of the heat sink. The transient plane source (TPS) method was used and compared with numerical simulations of polystyrene covered with an aluminum film with good agreements. The TPS method use a thin double nickel spiral, 10 µm thick, sandwiched between two layers of Kapton (polyimide film), each 25 µm thick, in contact with the material sample on both sides. The spiral serves both as the heat source and as a resistance thermometer and register the temperature increase in the material during a defined time period. The temperature increase in the sensor can then be used to calculate the thermal properties of the material.

4.5 Production

There are a number of producers that supply the VIP producers with the metalized multi-layered polymer laminate film. Brunner et al. (2006) described and investigated two of the laminates available at that time. The two laminates contained a number of different layers with polyethylene terephtalate (PET), aluminum, polyurethane (PUR) and low density polyethylene (LDPE). The thickness of the aluminum layer was only 30-100 nm and the PET was 12 µm. Between the metalized LDPE and metalized PET, 2 µm PUR was placed as a gluing layer. The aluminum was coated onto the PET layers using a vacuum web coating process where the aluminum was evaporated by a resistance heater and deposited on the PET film while in contact with a cooled drum. The process was a batch process from roll to roll that took place in a pressure chamber at a vacuum of 10^{-4} mbar (Ludwig et al., 2005). Three layers of metalized PET were used in the finished laminate.

Fumed silica has been produced on large scale since 1944 and is used as filling agent in lubricants, lacquers, paints, glues and medicines. The production is based on hydrolysis of silicon tetrachloride, $SiCl_4$, which means it is vaporized in a 1 000°C hydrogen flame reacting with oxygen, forming SiO_2. The byproduct is hydrochloric acid which can be used in industrial processes. The properties of the fumed silica can be changed by regulating the flame temperature, concentration of reactants and reaction time (Prodexim, n.d.).

To increase the workability of the fumed silica as a core material in VIP some additives are used. One substance used is the silicon carbide, SiC, which acts as an opacifier, lowering the heat transfer by radiation in the core. Silica sand and carbon are heated up to 1 700°C when they react and form silicon carbide. To increase the binding of the core material, cellulose fibers or polymer filaments are added to the mixture. The finished core material is composed of around 50-100% fumed silica, 1-20% silicon carbide and 1-12% fiber material (Microtherm, 2009).

The final VIP component is to a large extent produced by a manual production process where each step involves manual handling by the production team. Fumed silica is mixed with the opacifier and fiber material and the mixture is pressed and cut to a sheet with appropriate size and form. The sheet is then dried in an oven until excess moisture has evaporated. The dry core material is wrapped in the laminate which is folded making three sides open. Two of the sides are heat sealed to close the openings and the panel is placed in a vacuum chamber for some time. When the pressure is below 1 mbar, the last open side of the panel is heat sealed and the VIP is ready for storage before delivery. After around three weeks, the internal pressure is measured and if it exceeds 3 mbar, the panel is recycled. Panels with a pressure below 3 mbar is delivered to the costumer (Bock, 2011).

4.6 Applications

Among the first applications of VIP was in refrigerators, freezers and cold shipping boxes where the space for insulation is limited. Several million VIP are produced each year and the largest market is in Japan where around 50% of the production and consumption takes place (Binz et al., 2005). Refrigerators have an expected service life of around 15 years which lowers the demands on the longtime durability of the panels. Therefore, often glass wool VIP is used in the refrigerator industry.

During 2002-2005, an international research team investigated the possibilities to use VIP in buildings. Researchers from Switzerland, Germany, France, the Netherlands, Sweden and Canada worked together in the IEA/ECBCS Annex 39 High Performance Thermal Insulation (HiPTI). In total 20 constructions were built or retrofitted and the consequences on energy use, thermal bridges and building physics were analyzed. The research team concluded that VIP has become a feasible and important mean for building energy efficient buildings. There are obstacles to overcome, mainly with cost and issues with durability and quality assurance, before VIP can be introduced on a large scale in buildings (Binz et al., 2005).

Conventional insulation materials require a thicker building envelope than what is required when using VIP, therefore VIP is highly interesting to use when an old building is undergoing an energy retrofitting measure. However, VIP cannot be adopted on the construction site which requires detailed technical drawings of the construction. The durability of the product has to be considered and, as with all retrofitting measures, the moisture performance of the retrofitting measure has to be investigated. The energy and moisture performance of the construction should not be changed to a risky state in case a VIP is punctured.

Investigations of constructions of new and retrofitted buildings using VIP have been performed by different architects, engineers and researchers. Johansson (2012b) presents a literature overview of how VIP has been used in a number of different constructions, both in new buildings and in retrofitted old buildings.

5 Other thermal insulation materials

There are a number of different novel thermal insulation materials and components which are used in the building industry, such as foamglass, polyurethane (PUR), polyisocyanurate (PIR) and polystyrene with added graphite. Future materials could be based on novel nanomaterials mixed with conventional construction materials, such as concrete.

5.1 Polyurethane (PUR) and polyisocyanurate (PIR)

One possible solution to decrease the heat flow through an insulation material is to make it filled with a gas with lower conductivity than air. This demands either a closed pore system or some sealing around the insulation core to keep the gas inside the material. In polyurethane (PUR), the air has been exchanged to a blowing agent with a lower thermal conductivity than air. Examples of these gases are hydrofluorocarbons (HFC), carbon dioxide, CO_2, and cyclopentane, C_5H_{10}. The gas is trapped in the closed pore system of the PUR which is produced by a reaction between polyisocyanates and polyols. In case of fire, PUR will emit the substances hydrogen cyanide (HCN) and isocyanates which are poisonous (Jelle, 2011). The thermal conductivity of PUR is dependent on a number of factors such as density and moisture content, but for building applications it is generally around 24 mW/(m·K).

Polyisocyanurate (PIR) is an improvement of the polyurethane (PUR) by using other substances, reactants and catalysts in the production process. The result is a material which has a thermal conductivity around 22 mW/(m·K) (EcoTherm, 2010) and with improved fire performance compared to PUR. The PIR is coated on both sides with aluminium which can be covered by different facing materials (Kingspan, 2010).

PUR and PIR can be moulded as a board material and used as insulation in roofs, plastered walls, sandwich walls and floors. The properties are similar to EPS which make it possible to use in constructions where EPS traditionally have been used. However, when cutting PIR some dust is emitted which might be a health hazard and irritating to the skin and respiratory system. The PIR is also aging and by the diffusion of gases the thermal conductivity increases by time. Another problem is the shrinkage of the PIR of up to 1% which can create air gaps between the panels.

5.2 Graphite polystyrene

Expanded polystyrene (EPS) and extruded polystyrene (XPS) have been used in building industry for many years. The EPS is produced from polystyrene which is expanded by e.g. pentane C_5H_{12} to form a rigid board. Another production method is used to produce the XPS where the polystyrene is produced through a nozzle which releases the pressure causing the material to expand. The gases which are used to expand the XPS are e.g. hydrofluorocarbons (HFC), carbon dioxide, CO_2, and pentane, C_5H_{12} (Jelle, 2011). The thermal conductivity of the EPS and XPS is around 36 mW/(m·K).

Graphite polystyrene is an improvement of the EPS product where graphite is added to the mixture. The graphite lowers the thermal transfer by radiation through the pores in the EPS which leads to a reduction of the thermal conductivity to 31 mW/(m·K) which is approximately 20% lower than the conventional material. As is the case for EPS, the material shrinks after production which means it should be stored some time before integrated in the construction (BASF, 2011).

5.3 Materials of tomorrow

Jelle (2011) presented a summary of the conventional and novel thermal insulation materials and components available today together with an outlook on what can be developed in the future. A component which is available today but with questionable future outlook is the gas filled panels (GFP). The GFP is produced by removing the air from a panel with an internal honeycomb structure and replacing it with a less conductive gas such as argon, krypton and xenon. The component has similarities with the VIP but require a less advanced core and envelope material since the component does not have to withstand the atmospheric gas pressure on the envelope. However, the gas conductivity is much higher than in VIP where the gas is evacuated. The heat transfer by radiation is minimized by using coatings with a high emissivity on the internal surfaces. The theoretical thermal conductivity is lower than the 40 mW/(m·K) which has been measured in lab.

For the future thermal insulation material, Jelle (2011) predicted great possibilities using custom made nanomaterials as thermal insulation. A range of new materials are proposed such as vacuum insulation materials (VIM), nano insulation materials (NIM), gas insulation materials (GIM) and dynamic insulation materials (DIM). Development of these materials has just started and the future will tell which material or component that will be used in the buildings of tomorrow. The physical properties of the future materials should be as good or better than VIP, but without its disadvantages.

The VIP cannot be cut on site; it is vulnerable to mechanical influence and diffusion of air and moisture. VIM is similar to VIP but has a closed pore structure instead of the protective envelope. It is a challenge to keep the vacuum in the VIM during the entire service life (Jelle, 2011).

An alternative to the VIM discussed above, is the GIM which is similar to VIM but with a gas filling. GIM will probably have a longer service life than VIM since the pore structure will not be exposed to the same pressure difference (Jelle, 2011).

The most remote material is the NIM which is a development of the VIP but without the envelope. The pores in the NIM should be around 40 nm which means the Knudsen effect will have a substantial influence on the gas conduction in the material, see Figure 2.3. To create the low thermal conductivity of the material, the conduction through the solid and radiation have to be minimized. If the low thermal conductivity can be achieved the NIM could be the material of tomorrow (Jelle, 2011).

DIM should actively control the thermal conductivity of the material either by varying the internal gas pressure, the emissivity in the material or the conduction through the solid. The DIM should work in a similar way as electrochromic and phase change materials, i.e. adapting to the changes in the surrounding climate (Jelle, 2011).

6 Summary and comparison of the materials

This report has presented a survey of different thermal insulation materials components. With the knowledge of the basic heat transfer mechanisms and the ways to reduce the total thermal conductivity of a material or component, novel thermal insulation materials and components were described. A summary of the thermal conductivity of the materials is presented in Table 6.1.

Table 6.1. Thermal conductivity of the materials discussed in the report.

Material	Thermal conductivity (mW/(m·K))
Opaque aerogel	13-20
Transp. aerogel (evac/ambient)	10*/17-20*
VIP (evac/puntured)	4/20
EPS	36
XPS	34
EPS w. graphite	31
PUR	24
PIR	22
Render w. aerogel	25

*Apparent conductivity

Aerogels are still in development. The production is energy consuming which makes it expensive and problematic from an energy saving perspective, although alternative ways of production are investigated to reduce the energy use.

For windows, evacuated aerogels can lower the thermal losses significantly but evacuation will create problems of sealing and thermal bridges as discussed for VIP. For atmospheric pressure windows, the aerogel does not perform better than triple glazing windows for the same solar transmittance. The transparent aerogels could although function as insulation around solar collectors to increase their efficiency by reducing heat losses.

There are some promising formats of opaque aerogels. Aerogel blankets are flexible and easy to mount, even for complex geometries. The blankets can be cut and adjusted at the building site. Render with aerogel addition could replace the render on old façades. This would give the benefits of exterior insulation without change in the appearance of the building.

The use of VIP is viable in floors, ceilings and walls. It is important to educate the staff working with VIP of the importance of careful handling and knowledge of the consequences of a destroyed panel. A specialist should be present during the entire planning and installation process. The VIP must be well protected against any mechanical damages since the energy efficiency of the construction is heavily reduced in case the VIP is punctured. The cost of VIP is still too high to implement in ordinary housing projects, the additional cost can be justified with space savings and in buildings with cultural values. As the production methods develop and the amount of VIP produced increases, the cost might go down.

7 References

Aerogel. (2012). Available at: <www.aerogel.org> [Accessed March 1, 2012].

AGA. (1985). *Gas Handbook*, Uppsala: Almquist & Wiksell. ISBN: 91-970061-1-4.

Baetens, R., Jelle, B.P. & Gustavsen, A. (2010). Aerogel insulation for building applications: A state-of-the-art review. *Energy and Buildings*, 43, pp.761-769.

BASF. (2011). Neopor Wall Insulation. Ludwigshafen, Germany: BASF SE.

Binz, A., Moosmann, A., Steinke, G., Schonhardt, U., Fregnan, F., Simmler, H., Brunner, S., Ghazi, K., Bundi, R., Heinemann, U., Schwab, H., Cauberg, J. J. M., Tenpierik, M. J., Jóhannesson, G. A., Thorsell, T. I., Erb, M., and Nussbaumer, B. (2005). *Vacuum Insulation in the Building Sector. Systems and Applications (Subtask B)*: IEA/ECBCS Annex 39 High Performance Thermal Insulation (HiPTI).

Bock, T. (2011). Study visit at va-Q-tec production facility in Wuerzburg, Germany, June 10, 2011.

Boverket. (2010). *Energi i bebyggelsen - tekniska egenskaper och beräkningar - resultat från projektet BETSI*. Karlskrona, Sweden: Boverket.

Brodt, K. H. (1995). *Thermal insulation: CFC-alternatives and vacuum insulation (Dissertation)*. Delft, The Netherlands: Delft University of Technology, Faculty of Applied Physics.

Brodt, K. H. and Bart, G. C. (1994). Performance of sealed evacuated panels as thermal insulation. *International Journal of Refrigeration, 17*(4), 257-262.

Brunner, S., Gasser, P., Simmler, H., and Wakili, K. G. (2006). Investigation of multilayered aluminium-coated polymer laminates by focused ion beam (FIB) etching. *Surface and Coatings Technology, 200*(20-21), 5908-5914.

Brunner, S., Tharian, P. J., Simmler, H., and Ghazi Wakili, K. (2008). Focused ion beam (FIB) etching to investigate aluminium-coated polymer laminates subjected to heat and moisture loads. *Surface and Coatings Technology, 202*(24), 6054-6063.

Caps, R. (2005). Monitoring Gas Pressure in Vacuum Insulation Panels. *Proceedings of the 7th International Vacuum Insulations Symposium*, September 28-29, 2005, Duebendorf/Zurich, Switzerland. pp. 57-66.

Caps, R. & Fricke, J. (1986). Infrared radiative heat transfer in highly transparent silica aerogel. *Solar Energy*, 36(4), pp.361–364.

EcoTherm. (2010). Eco-Cavity COSHH Hazard Datasheet. Basildon, UK: EcoTherm® Insulation (UK) Ltd.

Engel, T. & Reid, P. (2006). *Physical Chemistry*, San Fransisco: Benjamin Cummings. ISBN: 0-8053-3842-X.

Erbenich, G. (2009). How to Identify a High Quality VIP: Methods and Techniques to Guarantee High Quality Production and Application. *Proceedings of the 9th International Vacuum Insulation Symposium*, September 18-19, 2009, London, UK.

European Commission. (2008). *Communication from the Commission to the European Parliament, the Council, the European Economic and Social Committee and the Committee of the Regions - 20 20 by 2020 - Europe's climate change opportunity*. Available at <http://eur-lex.europa.eu/LexUriServ/LexUriServ.do?uri=CELEX:52008DC0030:EN:HTML:NOT>.

Fricke, J., Heinemann, U., and Ebert, H. P. (2008). Vacuum insulation panels - From research to market. *Vacuum, 82*(7), 680-690.

Fricke, J., Lu, X., Wang, P., Büttner, D. & Heinemann, U. (1992). Optimization of monolithic silica aerogel insulants. *International journal of heat and mass transfer*, 35(9), pp.2305–2309.

Garnier, G., Marouani, S., Yrieix, B., Pompeo, C., Chauvois, M., Flandin, L., and Brechet, Y. (2011). Interest and durability of multilayers: from model films to complex films. *Polymers for Advanced Technologies, 22*(6), 847-856.

Ghazi Wakili, K., Bundi, R., and Binder, B. (2004). Effective thermal conductivity of vacuum insulation panels. *Building Research and Information, 32*(4), 293-299.

Ghazi Wakili, K., Stahl, T., and Brunner, S. (2011). Effective thermal conductivity of a staggered double layer of vacuum insulation panels. *Energy and Buildings, 43*(6), 1241-1246.

Grynning, S., Jelle, B. P., Uvsløkk, S., Gustavsen, A., Baetens, R., Caps, R., and Meløysund, V. (2011). Hot box investigations and theoretical assessments of miscellaneous vacuum insulation panel configurations in building envelopes. *Journal of Building Physics, 34*(4), 297-324.

Hümmer, E., Rettelbach, T., Lu, X. & Fricke, J. (1993) Opacified silica aerogel. *Thermochimica Acta*, 218, pp.269–276.

Iler, R.K. (1979). Chapter 5: Silica Gels and Powders. In *Chemistry of Silica - Solubility, Polymerization, Colloid and Surface Properties and Biochemistry*. John Wiley & Sons, pp. 462–621, ISBN: 978-1-60119-117-5. Available at: <http://www.knovel.com>.

Jelle, B. P. (2011). Traditional, state-of-the-art and future thermal building insulation materials and solutions - Properties, requirements and possibilities. *Energy and Buildings, 43*(10), 2549–2563.

Jelle, B. P., Gustavsen, A., and Baetens, R. (2009). Beyond vacuum insulation panels - How may it be achieved? *Proceedings of the 9th International Vacuum Insulation Symposium*, September 18-19, 2009, London, UK.

Johansson, P. (2012a). *Retrofitting of old Exterior Wall with Vacuum Insulation Panels: Meaurements of Thermal Properties, Moisture Performance and Practical Considerations* (Lic. Thesis 2012:2). Gothenburg, Sweden: Chalmers University of Technology, Department of Civil and Environmental Engineering.

Johansson, P. (2012b). *Vacuum Insulation Panels in Buildings: Literature Review* (Report 2012:1). Gothenburg, Sweden: Chalmers University of Technology, Department of Civil and Environmental Engineering.

Johansson, P., Adl-Zarrabi, B., and Hagentoft, C.-E. (2012). Using Transient Plane Source Sensor for Determination of Thermal Properties of Vacuum Insulation Panels. *Proceedings of the 5th International Building Physics Conference*, May 28-31, 2012, Kyoto, Japan.

Kingspan. (2010). Kooltherm Product Safety Information. Herefordshire, UK: Kingspan Insulation Ltd.

Kirkbir, F., Murata, H., Meyers, D. & Chaudhuri, S. (1998) Drying of aerogels in different solvents between atmospheric and supercritical pressures. *Journal of non-crystalline solids*, 225, pp.14–18.

Kistler, S.S. (1931a). Coherent expanded aerogels and jellies. *Nature*, 127, p.741.

Kistler, S.S. (1931b). Coherent expanded Aerogels. *Journal of Physical Chemistry*, 36(1), pp.52-64.

Ludwig, R., Kukla, R., and Josephson, E. (2005). Vacuum Web Coating - State of the Art and Potential for Electronics. *Proceedings of the IEEE, 93*(8), 1483-1490.

Microtherm. (2009). SlimVac Safety Data Sheet. Sint-Niklaas, Belgium: Microtherm N V.

Morel, B., Autissier, L., Autissier, D., Lemordant, D., Yrieix, B., and Quenard, D. (2009). Pyrogenic silica ageing under humid atmosphere. *Powder Technology, 190*(1-2), 225-229.

Mukhopadhyaya, P., Kumaran, K., Normandin, N., van Reenen, D., and Lackey, J. (2008). High-Performance Vacuum Insulation Panel: Development of Alternative Core Materials. *Journal of Cold Regions Engineering, 22*(4), 103-123.

Nilsson, O., Fransson, Å. & Sandberg, O. (1986). Thermal properties of silica aerogel. In *Aerogels*. Springer Proceedings in Physics. Berlin: Springer-Verlag, pp. 121–132, ISBN: 3-540-16256-9.

NIST. (2011). *NIST Chemistry WebBook*, NIST. Available at: <http://webbook.nist.gov/chemistry/> [Accessed February 7, 2012].

Parmenter, K.E. & Milstein, F. (1998). Mechanical properties of silica aerogels. *Journal of non-crystalline solids*, 223(3), pp.179–189.

Parvathy Rao, A., Pajonk, G.M. & Rao, A.V. (2005). Effect of preparation on the physical and hydrophobic properties of two step processed ambient pressure dried silica aerogels. *Journal of materials science*, 40(13), pp.3481–3489.

Petersson, B.-Å. (2007). *Tillämpad byggnadsfysik* 3rd ed., Studentlitteratur. ISBN: 978-91-44-04886-4.

Porextherm. (2009). Vacupor NT-B2 Version 1.01 / 12-22-09. Kempten, Germany: Porextherm Dämmstoff GmbH.

Prodexim. (n.d.). *Fumed Silica*. London, UK: Prodexim UK Ltd. Available at: <http://www.prodexim.com/en/products/chemical/Fumed-Silica.html> [Accessed January 24, 2012].

Reim, M. et al. (2004). Silica-aerogel granulate–Structural, optical and thermal properties. *Journal of non-crystalline solids*, 350, pp.358–363.

Rubin, M. & Lampert, C.M. (1983). Transparent silica aerogels for window insulation. *Solar Energy Materials*, 7(4), pp.393–400.

Scheuerpflug, P., Caps, R., Buttner, D. & Fricke, J. (1985). Apparent thermal conductivity of evacuated SiO2-aerogel tiles under variation of radiative boundary conditions. *International journal of heat and mass transfer*, 28(12), pp.2299–2306.

Schonhardt, U., Binz, A., Wohler, M., and Dott, R. (2003). *Ökobilanz eines Vakuum-Isolations-Paneels (VIP)*. Muttenz, Switzerland: Institut für Energie, Fachhochschule beider Basel.

Schreiber, E., Boy, E. & Bertsch, K. (1986). Aerogel as a tyransparent thermal insulation material for buildings. In *Aerogels*. Springer Proceedings in Physics. Berlin: Springer-Verlag, pp. 133–139, ISBN: 3-540-16256-9.

Schwab, H., Stark, C., Wachtel, J., Ebert, H.-P., and Fricke, J. (2005). Thermal Bridges in Vacuum-insulated Building Façades. *Journal of Thermal Envelope & Building Science, 28*(4), 345-355.

Simmler, H., Brunner, S., Heinemann, U., Schwab, H., Kumaran, K., Mukhopadhyaya, P., Quénard, D., Sallée, H., Noller, K., Kücükpinar-Niarchos, E., Stramm, C., Tenpierik, M. J., Cauberg, J. J. M., and Erb, M. (2005). *Vacuum Insulation Panels. Study on VIP-components and Panels for Service Life Prediction of VIP in Building Applications (Subtask A)*: IEA/ECBCS Annex 39 High Performance Thermal Insulation (HiPTI).

Soleimani Dorcheh, A. & Abbasi, M. (2008). Silica aerogel; synthesis, properties and characterization. *Journal of materials processing technology*, 199(1-3), pp.10–26.

Stahl, T., Brunner, S., Zimmermann, M., and Ghazi Wakili, K. (2012). Thermo-hygric properties of a newly developed aerogel based insulation rendering for both exterior and interior applications. *Energy and Buildings, 44*(0), 114-117.

Stepanian, C., Gould, G. & Begag, R. (2006) Aerogel composite with fibrous batting. Pat. No. US 7,504,346.

Svendsen, S. (1992). Solar collector with monolithic silica aerogel. *Journal of non-crystalline solids*, 145, pp.240–243.

Tamon, H., Sone, T. & Okazaki, M. (1997). Control of Mesoporous Structure of Silica Aerogel Prepared from TMOS. *Journal of Colloid and Interface Science*, 188(1), pp.162-167.

Tillotson, T.M. & Hrubesh, L.W. (1992). Transparent Ultralow-density silica aerogels prepared by a two-step sol-gel process. *Journal of non-crystalline solids*, 145, pp.44-50.

Willems, M. K., Schild, K., and Hellinger, G. (2005). Numerical investigation on thermal bridge effects in vacuum insulating elements. *Proceedings of the 7th International Vacuum Insulation Symposium*, 145-152.